nature structural & molecular biology

Mapping the interaction surface of linker histone $H1^0$ with the nucleosome of native chromatin *in vivo*

David T Brown[1], Tina Izard[2] & Tom Misteli[3]

H1 linker histones stabilize the nucleosome, limit nucleosome mobility and facilitate the condensation of metazoan chromatin. Here, we have combined systematic mutagenesis, measurement of *in vivo* binding by photobleaching microscopy, and structural modeling to determine the binding geometry of the globular domain of the $H1^0$ linker histone variant within the nucleosome in unperturbed, native chromatin *in vivo*. We demonstrate the existence of two distinct DNA-binding sites within the globular domain that are formed by spatial clustering of multiple residues. The globular domain is positioned via interaction of one binding site with the major groove near the nucleosome dyad. The second site interacts with linker DNA adjacent to the nucleosome core. Multiple residues bind cooperatively to form a highly specific chromatosome structure that provides a mechanism by which individual domains of linker histones interact to facilitate chromatin condensation.

The basic subunit of eukaryotic chromatin is the nucleosome, which consists of the chromatosome and additional linker DNA[1]. The chromatosome is comprised of ~168 bp of DNA, an octamer of core histones and one molecule of linker or H1 histone[2,3]. Linker histones act to stabilize the nucleosome and to facilitate folding of nucleosomal arrays into higher-order structures[4–7]. In higher organisms, linker histones have a conserved structure consisting of a central globular domain flanked by a long, lysine-rich C-terminal tail and a shorter, often basic N-terminal extension[8]. Specific subdomains of the C-terminal tail are crucial for H1–linker DNA binding and for stabilizing folded chromatin structures[9–11]. The central globular domain protects the chromatosome from nuclease digestion, and specific interactions of this domain within the chromatosome are likely to substantially influence the structural geometry of condensed chromatin[2,12,13]. Binding of the globular domain also has direct effects on gene expression at the nucleosomal level[14–16]. The central globular domain is believed to bind at or near the nucleosome dyad and to contact at least two strands of DNA[17–20]. Inspection of the crystal structure of the globular domain of the H5 linker histone variant (GH5) in the absence of DNA has suggested the existence of two well-separated DNA-binding sites[21]. Accordingly, simultaneous mutation of the residues in these sites abolishes the ability of GH5 to bind linker histone–depleted oligonucleosomes[19] or reconstituted mononucleosomes *in vitro*[20]. However, the precise interaction surface and the position of H1 on the nucleosome *in vivo* remain unknown, which makes it difficult to determine the way in which H1 functionally influences chromatin structure and gene expression[12,13].

Fluorescent recovery after photobleaching (FRAP) has recently been developed as a powerful tool to quantitatively measure the binding of proteins to unperturbed chromatin in living cells[22–25]. These analyses have shown that both mouse and human H1 isoforms bind dynamically to chromatin *in vivo* with a residence time on the order of minutes and that both the globular and C-terminal domains are required for high-affinity H1 binding[22,23]. Here, we have applied FRAP to a comprehensive collection of H1 mutants to identify specific residues within the globular domain of the mouse $H1^0$ linker histone variant that contribute to nucleosomal binding. Mapping of these residues onto the atomic structure of the globular domain defined the *in vivo* interaction surface of H1 with the nucleosome, and using molecular modeling, we determined the position of the linker histone within the chromatosome. The observed binding geometry suggests a mechanism wherein the globular and C-terminal domains of H1 interact to facilitate chromatin condensation.

RESULTS

Identification of H1 binding residues using FRAP

To identify the residues within the globular domain that are involved in nucleosomal contacts *in vivo*, we generated a comprehensive set of H1–green fluorescent protein (GFP) fusion constructs containing individual point mutations in the murine $H1^0$ variant. Within the globular domain, this subtype is 97% homologous to the well-characterized avian H5 variant[26]. First, simultaneous point mutations were introduced at each of the putative DNA-contact sites within the globular domain that have been suggested by *in vitro* analyses[20] (**Fig. 1a**). The basic residues in the primary site (Lys69, Lys73 and Lys85), secondary site (Lys40, Arg42, Lys52 and Arg94) or both were simultaneously replaced with alanine, and the binding of the mutants was determined by FRAP in stable cell lines. All experiments were

[1]Department of Biochemistry, University of Mississippi Medical Center, Jackson, Mississippi 39216, USA. [2]Department of Hematology-Oncology, St. Jude Children's Research Hospital, Memphis, Tennessee 38105, USA. [3]National Cancer Institute, US National Institutes of Health (NIH), Bethesda, Maryland 20892, USA. Correspondence should be addressed to D.T.B. (dbrown@biochem.umsmed.edu) or T.M. (mistelit@mail.nih.gov).

Received 10 November 2005; accepted 9 December 2005; published online 5 February 2006; doi:10.1038/nsmb1050

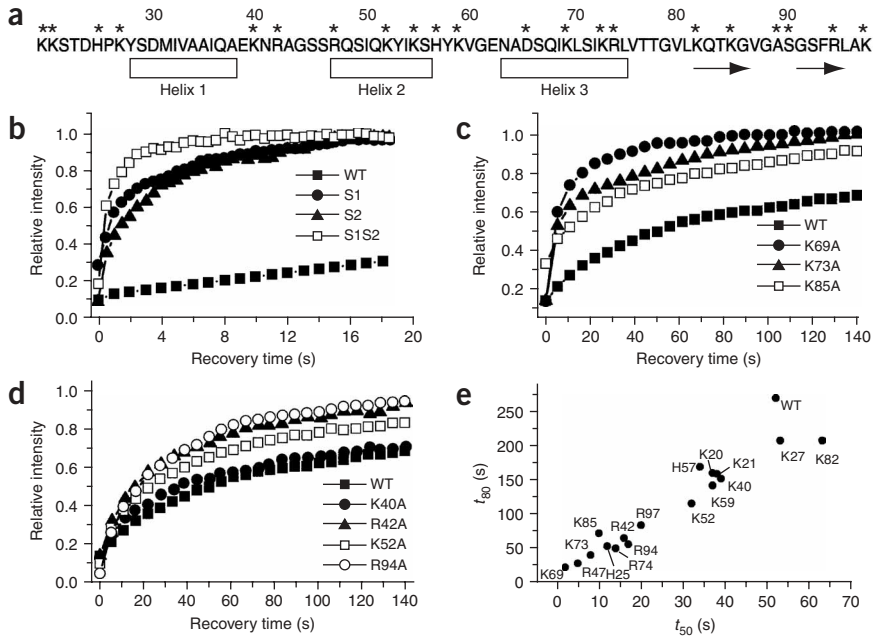

Figure 1 FRAP analysis of mutant and wild-type (WT) H1-GFP. (**a**) Sequence of the globular domain of $H1^0$. Residues are numbered from the initiator methionine to allow direct comparison to the H5 sequence. Asterisks indicate amino acids mutated in this study. Boxes and arrows below the sequence indicate α-helices and β-sheets, respectively, as determined from the crystal structure of H5 (ref. 21). (**b**) Quantitative FRAP analysis of stable transfectants expressing $H1^0$-GFP constructs containing multiple mutations in putative binding sites. S1, site 1 mutations, K69A K73A K85A; S2, site 2 mutations, K40A R42A K52A R94A; S1S2, all seven of these mutations. (**c**,**d**) Quantitative FRAP analysis of stable transfectants expressing H1-GFP constructs containing single mutations in putative binding residues. (**e**) FRAP results upon mutation of each basic residue in the globular domain to a neutral residue. Transfectants expressing these $H1^0$-GFP constructs were analyzed by FRAP to determine t_{50} and t_{80} (see **Table 1**). Values are averages from at least ten cells from three experiments. For clarity, error bars are omitted; typical standard deviations were below 10%.

performed using an optimized FRAP protocol and a standardized bleach region in euchromatin (see Methods for details). These multisite mutants showed very rapid recovery after photobleaching (**Fig. 1b**), indicating severely compromised binding[22]. The half-time for recovery, t_{50}, was used as a quantitative indicator of binding strength and was less than 1 s for all mutants but more than 50 s for the wild-type protein (**Fig. 1b** and **Table 1**). For comparison, t_{50} for nonbinding GFP alone is on the order of 380 ms under these conditions.

To determine the contributions of individual residues to binding, stable cell lines expressing constructs containing single point mutations of each residue were generated and analyzed by FRAP (**Fig. 1c**,**d**). Each mutant showed a recovery rate that was considerably faster than that of the wild-type protein (**Fig. 1c**,**d**). The strongest contributions to binding came from Lys69 and Lys73 ($t_{50} = 4$ s and 8 s, respectively), with intermediate contributions from Arg42 and Arg94 ($t_{50} = 16$ s and 17 s, respectively) and relatively weak contributions from Lys40 and Lys52 ($t_{50} = 39$ s and 28 s, respectively) (**Fig. 1c**,**d** and **Table 1**). Thus, the FRAP approach confirms the involvement of several residues previously implicated in DNA binding on the basis of *in vitro* assays, and it extends the *in vitro* assays by determining the relative contributions of single residues to binding *in vivo*.

To generate a complete map of the interaction surface of the globular domain of H1 within the nucleosome and to identify new residues that contribute to binding, we systematically generated mutants in each of the basic residues, including histidines, within the entire globular domain (**Fig. 1a**). Residues conserved between $H1^0$ and other variants were substituted with alanine, whereas nonconserved residues were replaced with the residue most commonly found in the other variants (**Table 1**). Analysis of the crystal structure of the H5 globular domain indicated that, with the exception of Lys55 (see **Supplementary Fig. 1** online), all of the mutated positively charged residues are oriented on or near the surface of the globular domain, where they could potentially interact with nucleosomal or linker DNA. For each mutant, stable cell lines were generated and their *in vivo* binding properties determined by FRAP (**Fig. 1e** and **Table 1**). Nine mutants had dramatically faster recovery rates with $t_{50} < 20$ s and $t_{80} < 90$ s (**Fig. 1e**). This group includes the previously identified lysines at positions 69, 73 and 85 in the putative primary interaction site and arginines 42 and 94 in the putative secondary site, as well as His25, which has been suggested to bind near the end of the chromatosome[27]. However, the data also identified three residues, Arg47, Arg74 and Lys97, that have not previously been implicated as

Table 1 Quantitative FRAP analysis of mutant H1 constructs

Genotype	t_{50} (sec)[a]	t_{80} (sec)[a]	Genotype	t_{50} (sec)	t_{80} (sec)
Wild type	52 ± 3.2	270 ± 7.3	D65K[b]	8 ± 0.3	46 ± 2.4
Site 1	1 ± 0.3	6 ± 1.1	K55D D65K[b]	47 ± 3.6	189 ± 12.5
Site 2	1 ± 0.4	8 ± 1.4	H57A	34 ± 2.8	169 ± 11.6
S12	<1	4.2 ± 0.8	H57E	28 ± 2.6	170 ± 10.8
K20A	37 ± 3.1	160 ± 5.2	K59A	37 ± 4.5	142 ± 8.2
K21A	38 ± 3.4	159 ± 6.5	K59D	37 ± 3.4	139 ± 9.6
H25G	12 ± 0.8	53 ± 2.3	E62H	76 ± 5.7	280 ± 10.2
H25E	10 ± 1.2	47 ± 4.1	K69A	4 ± 0.3	22 ± 1.6
H25K	32 ± 4.3	190 ± 8.6	K69R	23 ± 3.2	119 ± 7.5
K27T	53 ± 4.2	208 ± 12.1	K73A	8 ± 0.4	40 ± 2.8
K40A	39 ± 2.8	152 ± 9.5	K73E	4 ± 0.3	20 ± 3.1
K40E	34 ± 2.5	132 ± 9.1	K73R	49 ± 3.9	201 ± 11.9
R42A	16 ± 1.5	65 ± 3.2	R74A	14 ± 1.8	50 ± 3.1
R42E	10 ± 1.1	35 ± 2.2	K82V	63 ± 4.6	208 ± 12.7
R42K	45 ± 3.3	181 ± 9.2	Q83D	4 ± 0.3	17 ± 2.3
R47A	5 ± 0.2	28 ± 1.2	K85A	10 ± 1.1	72 ± 5.7
R47E	2 ± 0.3	20 ± 2.1	K85E	4 ± 0.3	18 ± 1.9
R47K	22 ± 2.2	121 ± 8.7	K85R	49 ± 4.2	197 ± 8.6
R47L	8 ± 0.5	41 ± 3.1	A89D	3 ± 0.2	19 ± 3.1
K52A	28 ± 1.6	120 ± 7.3	S90D	3 ± 0.2	21 ± 2.7
K55A[b]	12 ± 1.2	52 ± 3.8	R94A	17 ± 1.4	56 ± 2.6
K55E[b]	3 ± 0.2	20 ± 1.7	R97A	20 ± 1.3	84 ± 3.8
K55D[b]	5 ± 0.2	24 ± 1.3			

[a]Values for t_{50} and t_{80} were determined as previously described[24]. [b]See **Supplementary Figure 1**.

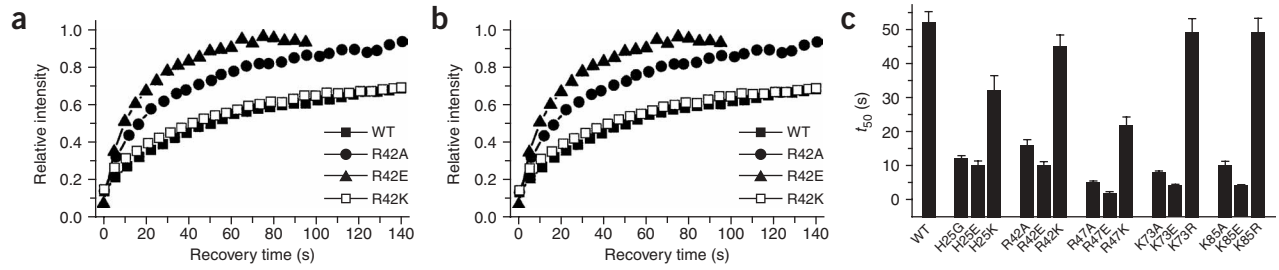

Figure 2 Electrostatically conservative mutations have much smaller effects on binding affinity. (**a**,**b**) FRAP analysis of cell lines expressing the indicated construct. (**c**) Selected FRAP results (**Table 1**). Values are averages from at least ten cells from three experiments. Error bars show s.d.

contributing to nucleosomal binding. Identical results were obtained for multiple clonal cell lines of each mutant construct (data not shown).

To validate this mutagenesis approach, we created additional mutants for the residues that showed the greatest effects (His25, Arg42, Arg47, Lys73 and Lys85). These basic residues were replaced one by one, either with glutamic acid to further weaken their potential for electrostatic interaction or with another basic residue, to determine whether their contributions to binding were due to electrostatic interaction. In all cases, replacement with glutamic acid further reduced binding (**Fig. 2**). In contrast, replacement with another basic residue resulted in greater binding activity than that observed after the neutral mutation and restored partial (His25, Arg47) or, in several cases (Arg42, Lys73, Lys85), nearly wild-type binding (**Table 1** and **Fig. 2**). The observed correlation between charge and binding behavior for all mutants is most consistent with these residues contributing electrostatic interactions with DNA to promote nucleosomal binding.

Biochemical confirmation of positioning

We wished to exclude the possibility that the measured FRAP kinetics of H1 mutants were due to aberrant binding to nonspecific sites resulting from tagging, mutagenesis or structural aberration of the protein. The overall properties of GFP-tagged H1 are indistinguishable from endogenous H1 by salt extraction and micrococcal nuclease (MNase) digestion analyses from reconstituted and isolated chromatin[22]. We confirmed that all H1 mutant proteins were structurally intact, in that all had circular dichroism spectra similar to that of the wild-type $H1^0$ globular domain (**Supplementary Fig. 2** online). Finally, we recently showed H1-GFP to be fully functional in somatic-cell nuclear transfer[28]. Therefore, these mutations and fusion to GFP do not introduce major changes in the structure or function of the globular domain of H1.

To conclusively demonstrate that mutant H1-GFP constructs are properly positioned on the nucleosome, we applied *in vivo* biochemical analysis. The most stringent assay for validating proper binding of H1 is protection of the chromatosome, a ~168-bp kinetic intermediate generated during MNase digestion of native chromatin[2,3]. Proper *in vivo* positioning of H1-GFP can be assayed and directly compared to that of untagged, endogenous H1 by separating mononucleosomes containing H1-GFP from those containing endogenous H1 on nucleoprotein gels after MNase digestion (**Fig. 3a**)[29]. Mononucleosome particles denoted as M3G consist of mononucleosomes containing $H1^0$-GFP, as demonstrated by the fluorescent signal, by the decreased migration expected to result from the increased mass of $H1^0$-GFP relative to H1 and by the absence of any DNA-containing material in the corresponding M3G region of ethidium bromide–stained mononucleosome samples from control cells not expressing $H1^0$-GFP (**Fig. 3a**). As expected in the case of proper *in vivo* positioning, the mononucleosomes containing H1-GFP contained ~168 bp of DNA, as did mononucleosomes containing endogenous H1 (**Fig. 3b**, M3). Mononucleosomes lacking H1 (M1), used as a control, contained DNA of ~148 bp. Notably, the mononucleosomes containing any of the H1-GFP mutants, with the exception of one (see below), contained DNA of ~168 bp, indistinguishable in size from that isolated from mononucleosomes with endogenous H1 or wild-type H1-GFP (**Fig. 3b**). Therefore, H1-GFP mutants are properly positioned, albeit with lower affinity, at their

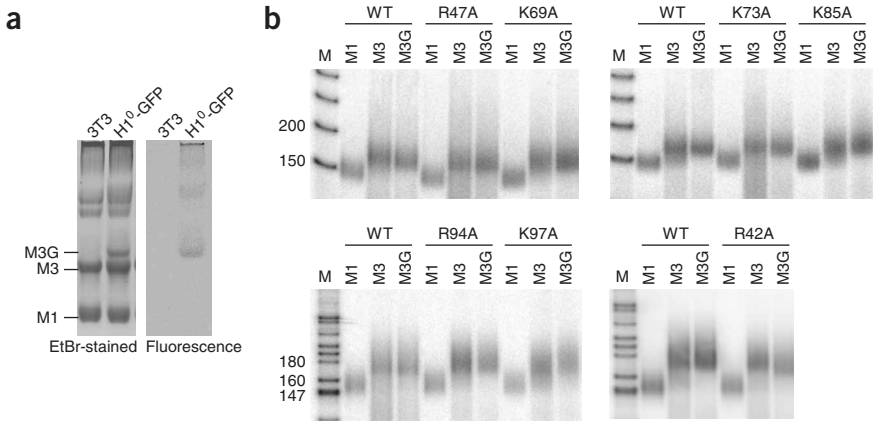

Figure 3 Mutant and wild-type H1-GFP proteins protect chromatosome-sized DNA. (**a**) Nuclei from parental 3T3 cells and transfectants expressing wild-type $H1^0$-GFP were digested with MNase. Soluble chromatin was separated into nucleoprotein particles and stained with ethidium bromide (left). Particles containing H1-GFP were visualized by fluorescence excitation (right). M3G, mononucleosomes containing H1-GFP; M3, mononucleosomes containing H1; M1, mononucleosomes lacking H1. The more slowly migrating material represents di- and higher-order chromatosomes[29]. (**b**) Nucleoprotein particles from cell lines expressing mutant and wild-type H1-GFP were separated on nucleoprotein gels, then excised and electroeluted, and purified, labeled DNA was separated by PAGE. For all mutants, the pattern and mobility of mononucleosome particles as visualized by fluorescence and ethidium bromide staining was identical to that of material from cells expressing wild-type H1-GFP.

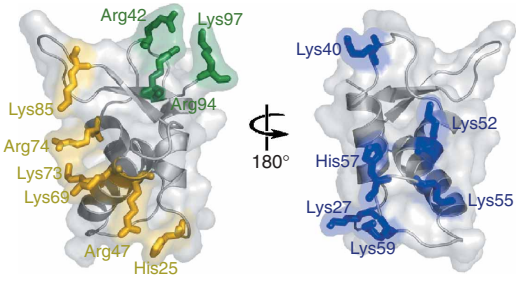

Figure 4 Map of the interaction surface of $H1^0$ based on data from **Table 1**. Yellow, binding residues in site 1; green, site 2; blue, nonbinding residues.

specific sites *in vivo*. The DNA isolated from mononucleosomes containing mutant R42A was consistently slightly shorter, as confirmed by analysis of the DNA by free acrylamide electrophoresis on internally calibrated lab chips (**Supplementary Fig. 3** online). Similar results have been obtained by *in vitro* studies of the binding of GH5 containing multiple mutations, including R42A, to oligonucleosomes[20]. Collectively, these results demonstrate that the mutant forms of H1-GFP confer protection of a discrete chromatosome-sized fragment of DNA. This would not be expected if these proteins were binding nonspecifically or atypically to linker DNA. We conclude that the mutant H1-GFP fusion proteins are specifically positioned on the nucleosome in the same manner as is the native protein and that their increased FRAP recovery rates reflect altered binding affinity.

Definition of two distinct binding sites

To define the interaction surface of the $H1^0$ globular domain with the nucleosome, we mapped the positions of the crucial residues onto the atomic structure of the H5 globular domain[21] (**Fig. 4**). The residues involved in binding are spatially clustered to form two distinct binding sites (**Fig. 4**). The larger, site 1, comprises His25, Arg47, Lys69, Lys73, Arg74 and Lys85; the smaller, site 2, comprises Arg42, Arg94 and Lys97. Notably, all of the binding residues in site 2 are located on flexible domains, possibly affording some latitude in binding geometry. Furthermore, all but one of the residues identified as nonbinding or as contributing little to the overall binding affinity were found to be located on a broad surface well separated from either binding site, on the opposite face of the domain (**Fig. 4**).

Positioning of H1 onto the nucleosome

To determine the geometry of H1 binding to the nucleosome by molecular modeling, we took advantage of the availability of the 2.8-Å crystal structure of the core nucleosome[30]. The globular domain of H5 was modeled onto the 2.8-Å crystal structure of the 147 base pairs of DNA associated with the nucleosome core[30] plus additional DNA to account for linker DNA associated with the chromatosome. To avoid potential bias regarding the nature of this additional DNA, modeling was performed on both straight and curved B-form DNA. The only assumptions in this approach are the experimentally verified properties that H1 binds at or near the nucleosome dyad[12,13], contacts the DNA in at least two sites[20] and protects 15–20 base pairs of chromatosomal DNA[2,3].

Using the surface map of the globular domain, we were able to generate a model that fits all of our experimental FRAP data as well as the published information on positioning (**Fig. 5**). The resulting H1-nucleosome model was then stereochemically refined using 200 rounds of coordinate energy minimization. In the resulting consensus model, binding site 1 interacts with one side of the DNA approximately one helical turn away from the nucleosome dyad. Helix 3, containing binding residues Lys69, Lys73 and Arg74, fits into the major groove in a manner similar to the recognition helices of several DNA-binding proteins with which H1 shares structural similarity[21,31]. The additional binding residues in site 1 (His25, Lys47 and Lys85) are positioned to interact favorably with the DNA backbone. These interactions are facilitated by the curvature of DNA as it wraps around the nucleosome. By contrast, attempts to accommodate all binding residues of the primary site, site 1, in a favorable binding orientation with straight or even slightly bent DNA were unsuccessful. Site 2, consisting of Arg42, Arg94 and Arg97, interacts with one of the entering-and-exiting linker DNA strands. The site of interaction is about 15 base pairs from the end of the nucleosomal core DNA, consistent with protection of chromatosomal DNA. Finally, all residues determined to play little or no role in binding are oriented away from DNA.

To experimentally validate this model, we selectively mutated several residues in the β-turn structure located at the C-terminal end of the globular domain. This region is highly conserved in sequence and structure among H1 variants in many species. Our model predicts that mutation of residues within the β-turn would severely compromise binding. Indeed, mutation of Ala89 or Ser90 to aspartate resulted in a t_{50} of 3 s for both mutants, compared to more than 50 s for the wild-type protein, in FRAP assays (**Table 1**). This loss of binding is consistent with the location of these residues near site 1 at the dyad.

DISCUSSION

We have derived the interaction surface and binding geometry of the globular domain of linker histone H1 bound to chromatin, on the basis of experimental binding data from living cells combined with molecular modeling approaches. These studies have defined two distinct binding sites on the H1 globular domain, site 1 and site 2, and we propose that they interact with the major groove near the dyad axis and with the minor groove on the linker DNA, respectively, an orientation that was confirmed by targeted mutagenesis.

Our model is compatible with available information regarding the organization of nucleosomes into higher-order chromatin structures.

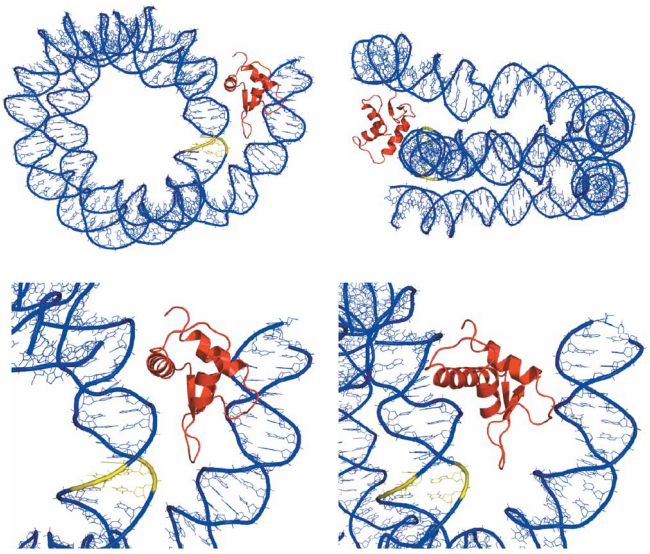

Figure 5 Molecular model of the location of H1 within the nucleosome. Blue, chromatosomal DNA; yellow, nucleosome dyad; red, the globular domain of H1.

Specifically, the binding residues in site 1 would be expected to be structurally well organized and therefore best suited for binding the conserved DNA structure found at the nucleosome dyad. In contrast, residues in site 2 are located in flexible domains that would allow some latitude in binding, to accommodate the more heterogeneous structures expected for linker DNA. This orientation of the globular domain of H1 would also place the N- and C-terminal tails of the molecule in favorable positions to interact with linker DNA distal to the chromatosome. An X-ray structure of a tetranucleosome, albeit reconstituted in the absence of linker histone, has recently been reported[32]. Remarkably, within the limits of resolution, our independently derived chromatosome structure is completely compatible with that of the tetranucleosome (**Supplementary Fig. 4** online).

On the basis of *in vitro* binding experiments, models for the position of GH5 in the nucleosome have suggested that a primary binding site (Lys69, Lys73 and Lys85) interacts with the entering-and-exiting DNA and that a secondary site (Lys40, Arg42, Lys52 and Arg94) interacts with DNA near the dyad[33,34]. In such a scenario, residues Lys40 and Lys52 are important for binding and orienting GH5 near the dyad. However, the *in vivo* FRAP assays indicate that these residues do not make major contributions to binding. The much larger size and shape of site 1 identified herein is very difficult to reconcile with a model in which this site binds the entering-and-exiting DNA, requiring rather drastic distortions of the path of the DNA. Indeed, such distortions are not compatible with the architecture of linker DNA–H1 interactions as seen in EM images of chromatin[6]. Finally, the slightly smaller size of the chromatosomal DNA of the R42A mutant is most consistent with the location of this residue near the end of one of the entering-and-exiting strands.

Our observations also suggest the intriguing hypothesis that the globular domains of individual H1 variants might have distinct binding geometries within the nucleosome, thereby contributing to chromatin heterogeneity[35,36]. In particular, residues His25, Arg47 and Arg74 are strong contributors to site 1 binding in $H1^0$, yet these residues are replaced by neutral and conserved residues in the other somatic H1 variants H1a through H1e[37]. Further, substitutions of the $H1^0$ binding residues with the conserved amino acids found in other H1 variants severely compromise $H1^0$ binding (**Table 1**). Finally, analysis of binding residues in variant H1c has revealed that several sites not conserved between H1c and $H1^0$ are indeed important for H1c binding (D.T.B., unpublished data).

The quantitative data obtained herein also suggest multiple cooperative interactions between numerous residues within the globular domain of H1 and nucleosomal DNA and/or proteins, including core histones. $H1^0$ mutants harboring multiple substitutions (**Table 1**), as well as those bearing deletions of entire binding domains[22], have t_{50} values of approximately 1 s, a value approaching that of free GFP in the nucleus. Therefore, they may be considered 'null' or nonbinding mutants. Nonetheless, there are multiple key residues that are extremely important to binding, as mutation of, for example, Arg47, Lys69 or Lys73 alone also results in a t_{50} value of only $\sim$3 s, which approaches the null phenotype. This indicates that the contributions of these residues to binding in the wild-type protein are not additive, but rather they act in a synergistic fashion to facilitate binding.

Deletion of the entire C terminus or specific single-residue substitutions within this domain result in severely reduced residence times of human H1.1, indicating that the C terminus of H1 also contributes to binding[10]. These results are consistent with a biophysical analysis of a collection of deletion mutants of $H1^0$ suggesting that specific subdomains of the C terminus stabilize the structures of locally folded chromatin[11]. After the initial low-specificity electrostatic binding of the C terminus to linker DNA, these subdomains acquire specific structures that contribute to chromatin condensation. Notably, the subdomain most important for this process is located immediately downstream from the secondary binding site of the globular domain and, in our model, would be well positioned to induce formation of an apposed linker DNA stem[6]. We suggest that the specific binding geometry of the globular domain may guide or orient the C-terminal domain into a structure conducive to chromatin condensation. In this view, structural pliability resulting from the intrinsic disorder of the H1 C terminus allows for efficient but nonspecific initial capture of H1 through binding to linker DNA. This then places the globular domain near the nucleosome and, perhaps through one-dimensional scanning, promotes efficient and highly stable specific binding. Establishing stable binding of the globular domain would then promote the acquisition of structure within the C-terminal domain that facilitates chromatin condensation.

METHODS

Constructs and cell lines. Plasmid $MTH1^0$GFPneo has been previously described[29]. In this plasmid, the coding sequence for enhanced GFP is fused to the C terminus of the coding region for $H1^0$, and expression is under control of the mouse metallothionein promoter. Point mutations were introduced with the QuikChange mutagenesis kit (Stratagene) or by introduction of annealed oligonucleotides between restriction sites. Constructs were introduced into mouse BALB/c 3T3, and multiple stable transfectants were isolated and analyzed as described in ref. 22. For FRAP assays, cultures were grown in the absence of inducer. Under these conditions, H1-GFP comprises less than 5% of the total H1 population[22].

FRAP assays. For FRAP, cells were plated and observed in LabTekII chambers (Nalgene). FRAP was performed on a Zeiss LSM 510 confocal microscope using the 488-nm line of an argon laser (nominal output 40 W, beam width at specimen 0.2 μm). All experiments were done at 37 °C, and imaging was done with a ×100 objective, NA1.3. Scanning was bidirectional at the highest possible rate using a ×3 zoom with a pinhole of 1 Airy unit. Bleaching was achieved using two consecutive bleach scans of 49 ms duration at maximal laser power. The bleached region was 69 × 69 pixels and excluded heterogeneous nuclear features such as nucleoli and heterochromatin foci. During the recovery period, 100 images (512 × 512 pixels) were recorded until the recovery signal reached a plateau. To avoid erroneous measurements due to nonspecific bleaching during normal imaging, intervals between images during the postbleach phase were spaced so as to maintain a constant number of images. Identical imaging settings (50% laser intensity, 0.1% attenuation) were used for all pre- and postbleach images. Normalized recovery rates were determined as described in ref. 38. All datasets consisted of at least ten cells per experiment and experiments were performed in triplicate.

Nucleoprotein analysis. Parental 3T3 cells and transfectants expressing $H1^0$-GFP constructs were treated with $ZnCl_2$ for 24–48 h before nuclei were isolated as previously described[29]. Nuclei were digested with 4 U ml^{-1} MNase (Sigma) for 15 min at 25 °C. The reaction was stopped and nuclei were lysed by incubation in 1 mM EDTA and 2 mM EGTA on ice for 15 min. Nuclear debris was pelleted by centrifugation at 13,000*g* for 15 min. Soluble chromatin was separated into nucleoprotein particles on 3.5% acrylamide/0.5% agarose gels containing 30% (v/v) glycerol exactly as described in ref. 39. Individual particles were excised from the nucleoprotein gels and electroeluted into dialysis bags. DNA was purified by phenol-chloroform extraction, labeled with [^{32}P]ATP (ICN) and polynucleotide kinase (NEB) and separated on 6% neutral polyacrylamide gels.

Molecular modeling. The crystal structures of the nucleosome[30] and the globular domain of the H5 linker histone variant (GH5)[21], together with our *in vivo* photobleaching microscopy and systematic mutagenesis data, were used as the starting point to generate a model of the H1–nucleosome complex. A homology model of the globular domain of $H1^0$ was built from the GH5 crystal structure by homology modeling using LOOK 3.0 (Molecular

Applications Group). The DNA of the nucleosome was extended using O^{40} to account for entering-and-exiting DNA associated with the chromatosome. The resulting H1–nucleosome model was then stereochemically refined by 200 rounds of coordinate energy minimization using CNS[41].

Note: Supplementary information is available on the Nature Structural & Molecular Biology website.

ACKNOWLEDGMENTS

We thank D. Yellajoshyula and E. George for experimental assistance and M. Bustin and D. Sittman for discussions and critical reading of the manuscript. This work was supported by grants from the US National Science Foundation to D.T.B. (MCB0235800) and from the NIH to T.I. T.M. is a Fellow of the Keith Porter Endowment for Cell Biology. This research was in part supported by the Intramural Research Program of the NIH, National Cancer Institute, Center for Cancer Research and by NIH grant RR016476 from the MFGN INBRE Program of the National Center for Research Resources.

COMPETING INTERESTS STATEMENT

The authors declare that they have no competing financial interests.

Published online at http://www.nature.com/nsmb/
Reprints and permissions information is available online at http://npg.nature.com/reprintsandpermissions/

1. Wolffe, A.P. *Chromatin: Structure and Function* 3rd edn (Academic Press, San Diego, USA, 1995).
2. Noll, M. & Kornberg, R.D. Action of micrococcal nuclease on chromatin and the location of histone H1. *J. Mol. Biol.* **109**, 393–404 (1977).
3. Simpson, R.T. Structure of the chromatosome, a chromatin particle containing 160 base pairs of DNA and all the histones. *Biochemistry* **17**, 5524–5531 (1978).
4. Thoma, F., Koller, T. & Klug, A. Involvement of histone H1 in the organization of the nucleosome and of the salt dependent superstructures of chromatin. *J. Cell Biol.* **83**, 403–427 (1979).
5. Ramakrishnan, V. Histone H1 and chromatin higher order structure. *Crit. Rev. Eukaryot. Gene Expr.* **7**, 215–230 (1997).
6. Bednar, J. *et al.* Nucleosomes, linker DNA, and linker histone form a unique structural motif that directs the higher-order folding and compaction of chromatin. *Proc. Natl. Acad. Sci. USA* **95**, 14173–14178 (1998).
7. Carruthers, L.M. & Hansen, J.C. The core histone N termini function independently of linker histones during chromatin condensation. *J. Biol. Chem.* **275**, 37285–37290 (2000).
8. Allan, J., Hartman, P.G., Crane-Robinson, C. & Aviles, F.X. The structure of histone H1 and its location in chromatin. *Nature* **288**, 675–679 (1980).
9. Allan, J., Mitchell, T., Harborne, N., Bohm, L. & Crane-Robinson, C. Roles of H1 domains in determining higher order chromatin structure and H1 location. *J. Mol. Biol.* **187**, 591–601 (1986).
10. Hendzel, M.J., Lever, M.A., Crawford, E. & Th'ng, J.P. The C-terminal domain is the primary determinant of histone H1 binding to chromatin *in vivo*. *J. Biol. Chem.* **279**, 20028–20034 (2004).
11. Lu, X. & Hansen, J.C. Identification of specific functional subdomains within the linker histone $H1^0$ C-terminal domain. *J. Biol. Chem.* **279**, 8701–8707 (2004).
12. Thomas, J.O. Histone H1: location and role. *Curr. Opin. Cell Biol.* **11**, 312–317 (1999).
13. Travers, A.A. The location of linker histone in the nucleosome. *Trends Biochem. Sci.* **24**, 4–7 (1999).
14. Brown, D.T., Gunjan, A., Alexander, B.T. & Sittman, D.B. Differential effect of H1 variant overproduction on gene expression is due to differences in the central globular domain. *Nucleic Acids Res.* **25**, 5003–5009 (1997).
15. Vermaak, D., Steinback, O.C., Dimitrov, S., Rupp, R.A. & Wolffe, A.P. The globular domain of histone H1 is sufficient to direct specific gene repression in early *Xenopus* embryos. *Curr. Biol.* **8**, 533–536 (1998).
16. Cirillo, L.A. *et al.* Binding of the winged-helix transcription factor HNF3 to a linker histone site on the nucleosome. *EMBO J.* **17**, 244–254 (1998).
17. Staynov, D.Z. & Crane-Robinson, C. Footprinting of linker histones H5 and H1 on the nucleosome. *EMBO J.* **7**, 3685–3691 (1988).
18. Lambert, S. *et al.* Neutron scattering studies of chromatosomes. *Biochem. Biophys. Res. Commun.* **179**, 810–816 (1991).
19. Goytisolo, F.A. *et al.* Identification of two DNA-binding sites on the globular domain of histone H5. *EMBO J.* **15**, 3421–3429 (1996).
20. Duggan, M.M. & Thomas, J.O. Two DNA binding sites on the globular domain of histone H5 are required for binding to both bulk and 5 S reconstituted nucleosomes. *J. Mol. Biol.* **304**, 21–33 (2000).
21. Ramakrishnan, V., Finch, J.T., Graziano, V., Lee, P.L. & Sweet, R.M. Crystal structure of globular domain of histone H5 and its implications for nucleosome binding. *Nature* **362**, 219–223 (1993).
22. Misteli, T., Gunjan, A., Hock, R., Bustin, M. & Brown, D.T. Dynamic binding of histone H1 to chromatin in living cells. *Nature* **408**, 877–881 (2000).
23. Lever, M.A., Th'ng, J.P., Sun, X. & Hendzel, M.J. Rapid exchange of histone H1.1 on chromatin in living cells. *Nature* **408**, 873–876 (2000).
24. Phair, R.D. *et al.* Global nature of dynamic protein-chromatin interactions in vivo: three-dimensional genome scanning and dynamic interaction networks of chromatin proteins. *Mol. Cell. Biol.* **24**, 6393–6402 (2004).
25. Cheutin, T. *et al.* Maintenance of stable heterochromatin domains by dynamic HP1 binding. *Science* **299**, 721–725 (2003).
26. Pehrson, J.R. & Cole, R.D. Bovine $H1^0$ histone subfractions contain an invariant sequence which matches histone H5 rather than H1. *Biochemistry* **20**, 2298–2301 (1981).
27. Mirzabekov, A.D., Pruss, D.V. & Ebralidse, K.K. Chromatin superstructure-dependent crosslinking with DNA of the histone H5 residues Thr1, His25 and His62. *J. Mol. Biol.* **211**, 479–491 (1990).
28. Becker, M. *et al.* Differential in vivo binding dynamics of somatic and oocyte-specific linker histones in oocytes and during ES cell nuclear transfer. *Mol. Biol. Cell* **16**, 3887–3895 (2005).
29. Gunjan, A., Alexander, B.T., Sittman, D.B. & Brown, D.T. Effects of H1 histone variant overexpression on chromatin structure. *J. Biol. Chem.* **274**, 37950–37956 (1999).
30. Luger, K., Mader, A.W., Richmond, R.K., Sargent, D.F. & Richmond, T.J. Crystal structure of the nucleosome at 2.8 A resolution. *Nature* **389**, 251–260 (1997).
31. Clark, K.L., Halay, E.D., Lai, E. & Burley, S.K. Co-crystal structure of the HNF-3/fork head DNA-recognition motif resembles histone H5. *Nature* **364**, 412–420 (1993).
32. Schalch, T., Duda, S., Sargent, D.F. & Richmond, T.J. X-ray structure of a tetranucleosome and its implications for the chromatin fibre. *Nature* **436**, 138–141 (2005).
33. Zhou, Y.-B., Gerchman, S.E., Ramakrishnan, V., Travers, A. & Muyldermans, S. Position and orientation of the globular domain of linker histone H5 on the nucleosome. *Nature* **395**, 402–405 (1998).
34. Bharath, M.M., Chandra, N.R. & Rao, M.R. Molecular modeling of the chromatosome particle. *Nucleic Acids Res.* **31**, 4264–4274 (2003).
35. Alami, R. *et al.* Mammalian linker-histone subtypes differentially affect gene expression *in vivo*. *Proc. Natl. Acad. Sci. USA* **100**, 5920–5925 (2003).
36. Lee, H., Habas, R. & Abate-Shen, C. Msx1 cooperates with histone H1b for inhibition of transcription and myogenesis. *Science* **304**, 1675–1678 (2004).
37. Parseghian, M.H. & Hamkalo, B.A. A compendium of the histone H1 family of somatic subtypes: an elusive cast of characters and their characteristics. *Biochem. Cell Biol.* **79**, 289–304 (2001).
38. Phair, R.D. & Misteli, T. High mobility of proteins in the mammalian cell nucleus. *Nature* **404**, 604–609 (2000).
39. Huang, S.-Y. & Garrard, W.T. Electrophoretic analyses of nucleosomes and other protein-DNA complexes. *Methods Enzymol.* **170**, 116–142 (1979).
40. Jones, T.A., Zou, J.Y., Cowan, S.W. & Kjeldgaard, M. Improved methods for building protein models in electron density maps and the location of errors in these models. *Acta Crystallogr. A* **47**, 110–119 (1991).
41. Brunger, A.T. *et al.* Crystallography & NMR system: a new software suite for macromolecular structure determination. *Acta Crystallogr. D Biol. Crystallogr.* **54**, 905–921 (1998).